ACS APPLIED MATERIALS & INTERFACES

Research Article

www.acsami.org

Multifunctional g-C_3N_4 Nanofibers: A Template-Free Fabrication and Enhanced Optical, Electrochemical, and Photocatalyst Properties

Muhammad Tahir,[†] Chuanbao Cao,*[,†] Nasir Mahmood,[‡] Faheem K. Butt,[†] Asif Mahmood,[‡] Faryal Idrees,[†] Sajad Hussain,[†] M. Tanveer,[†] Zulfiqar Ali,[†] and Imran Aslam[†]

[†]Research Centre of Materials Science, Beijing Institute of Technology, Beijing 100081, P. R. China

[‡]Department of Materials Science and Engineering, Peking University, Beijing 100871, P.R. China

ABSTRACT: We have developed a facile, scale up, and efficient method for the preparation of graphitic-C_3N_4 nanofibers (GCNNFs) as electrodes for supercapacitors and photocatalysts. The as-synthesized GCNNFs have 1D structure with higher concentration of nitrogen that is favorable for higher conductivity and electrochemical performance. Secondly, the high surface area of GCNNF provides a large electrode−electrolyte contact area, sufficient light harvesting and mass transfer, as well as increased redox potential. Thus, the GCNNF supercapacitor electrode shows high capacitance of 263.75 F g^{-1} and excellent cyclic stability in 0.1 M Na_2SO_4 aqueous electrolyte with the capacitance retention of 93.6% after 2000 cycles at 1 A g^{-1} current density. GCNNFs exhibit high capacitance of 208 F g^{-1} even at 10 A g^{-1}, with the appreciable capacitance retention of 89.5%, which proves its better rate capability. Moreover, the GCNNF shows enhanced photocatalytic activity in the photodegradation of RhB in comparison to the bulk graphitic-C_3N_4 (GCN). The degradation rate constant of GCNNF photocatalyst is almost 4 times higher than GCN. The enhanced photocatalytic activity of GCNNF is mainly due to the higher surface area, appropriate bandgap, and fewer defects in GCNNF as compared to GCN. As an economical precursor (melamine) and harmless, facile, and template-free synthesis method with excellent performance both in supercapacitors and in photodegradation, GCNNF is a strong candidate for energy storage and environment protection applications.

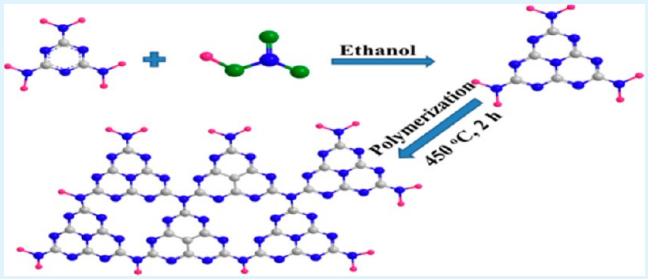

KEYWORDS: *nanofibers, carbon nitride, supercapacitors, photocatalyst, optical properties*

INTRODUCTION

One-dimensional (1D) nanostructures (wires, tubes, rods, belts, fibers, etc.) received vast interest after the discovery of carbon nanotubes due to their number of applications in the fields of microelectronics and optoelectronic devices, such as optical waveguides, field-effect transistors, and photodetectors.[1] 1D nanostructures exhibit excellent properties like field emission, gas sensing, photoconductivity, and phonon and electron transport properties since they possess a high surface-to-volume ratio and more active sites. 1D growth can also play an important role in improving the thermal, electrical, and mechanical properties of the materials.[2,3] The most familiar methods in which 1D nanostructures can be fabricated include X-ray lithography, proximal probe patterning, the direct and indirect vapor phase method, the chemical vapor deposition (CVD) method, strong $\pi-\pi$ self-assembly stacking, and electron beam.[4] However, fabrication of 1D graphitic carbon nitride (GCN) is still very difficult as its self-assembly process is very complicated.[4]

GCN is one of the most fascinating materials with excellent mechanical strength, thermal conductivity, water resistivity, and reliable chemical inertness, with major applications as a catalyst for organic synthesis, photoelectric converter, gas and fluorescent sensors, field emitters, electrode for fuel cells, and hydrogen storage material.[4−6] Different methods have been adopted to fabricate GCN like sol−gel, CVD, shock-wave compression, solvothermal method, polymer precursor's condensation, and pyrolysis.[4−10] There are few reports on fabrication of GCN 1D nanostructures like nanofibers, nanobelts, nanorods, nanotubes, and nanowires.[4−10] The aforesaid morphologies were obtained by using catalysts or via introduction of toxic and expensive chemicals. However, hard or soft templates were also used by a few groups to synthesize 1D GCN. Furthermore, the growth requires high temperature with a low yield of the product which is the major bottleneck to use GCN for real technological applications.[4−10] Therefore, it is necessary to develop a new template-free synthesis method which could produce a 1D nanostructure of GCN at the large scale and low temperature for its potential applications in diverse fields.

Supercapacitors, a class of energy storage devices, have fascinated the scientific community nowadays because of their long cycle life, rapid charge−discharge rate, low maintenance cost, and high power capability.[11] Supercapacitors are widely

Received: November 13, 2013
Accepted: December 20, 2013
Published: December 20, 2013

Scheme 1. Schematic Representation of Chemical Reaction for the Synthesis of GCNNF

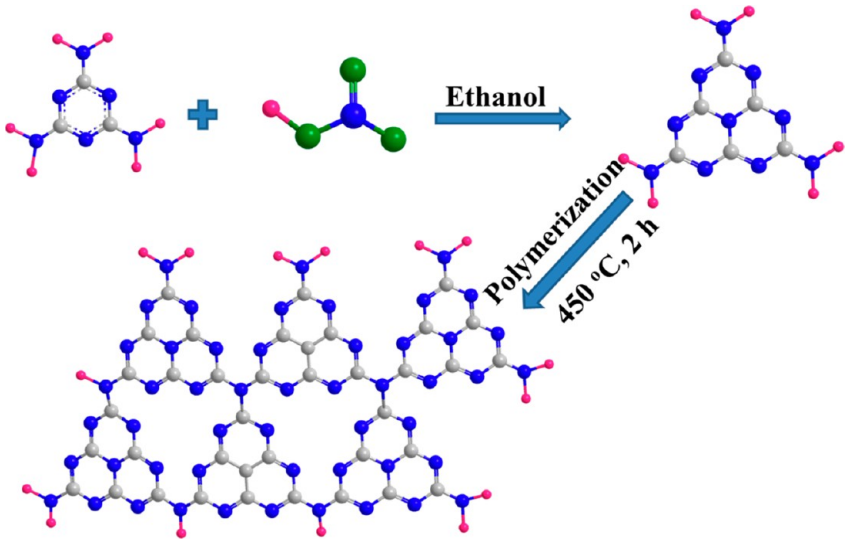

used in consumer electronics, electric vehicles, memory backup, industrial power management, and uninterrupted power sources, etc.[11] Furthermore, supercapacitors have less environmental impact and are safer than batteries.[12,13] The specific capacitance of supercapacitors basically depends on electrode material, thus the role of electrode materials is extremely important. There are arrays of electrode materials for supercapacitors, but carbon materials are most commonly used as electrode material due to their high conductivity, large surface area, stable physicochemical properties, varieties of forms, and plentiful sources.[14] However, their performance is not very good due to their low specific energy. Moreover, the inert surface of carbon materials makes it difficult for electrolyte to further penetrate into the internal layers of carbon. Different techniques have been used to overcome these problems like introduction of metal oxides, hetero atoms, and oxygen in carbon materials, but nitrogen doping seems to be the best way to deal with these issues.[15] The existence of nitrogen in carbonaceous materials improves capacity while maintaining excellent cyclability of supercapacitors, and it enhances the wettability and in consequence improves efficient utilization of the surface. However, doping of nitrogen is toxic and complex, and concentration of nitrogen is very low; also, special instruments and harsh conditions are required.[15,16] Therefore, a facile fabrication technique to assemble nitrogen-containing carbon materials for supercapacitors as electrodes with good performance is highly desirable. GCN is a potentially suitable candidate in this regard because of its high nitrogen content, easily tailorable structure, and low cost.[17]

Photocatalysts can separate harmful materials from water using solar energy. These photocatalysts needed to be easily separable, facile to fabricate, nontoxic in nature, low in cost, environmentally benign, and stable in water solutions.[6] A covalent GCN organic semiconductor with small bandgap, proper band positions, and controllable surface has been widely used as a metal-free energy transducer, in water splitting, in organic photosynthesis, and in environmental remediation.[6,18] However, there are some issues with GCN, which include: (1) high recombination rate of photogenerated electron−hole pair, (2) low surface area, and (3) poor mass diffusion that makes GCN less efficient for practical applications. Hence, it is essential to develop a physical or chemical procedure to modify GCN's optical, electronic, and textural properties to endorse photochemical reactions of GCN photocatalysis. Different methods have been adopted to resolve these issues, but morphological control of the GCN nanostructure seems to be the best way to deal with the aforesaid issues.[18−21] Nanostructured materials show better performance as compared to their corresponding bulk counterparts when functioning as a photocatalyst since it is an efficient way to promote charge movement and separation as well as mass diffusion through photoredox reactions .[18] Therefore, we fabricated nanofibers of GCN to take advantage of this size dependency in photocatalysts.

We have designed a safe and facile chemical route to fabricate nanofiber (NF)-like structures of GCN. These GCNNFs can scale-up with ease. These GCNNFs were for the first time used for the electrodes of supercapacitors in Na_2SO_4 electrolytes. The specific capacitance of the GCNNF supercapacitor electrode is 263.75 F g^{-1} at a current density of 1 A g^{-1}. The specific capacitance of GCNNF is much higher than other carbon-based materials. Photodegradation of RhB is also performed by using GCNNF and GCN. As-synthesized GCNNF exhibits high surface area, suitable bandgap, and less crystal defects which are useful for photodegradation of RhB. Moreover, the used catalyst is successfully recovered and reused three times without apparent loss of selectivity that confirmed the extraordinary high reproducibility of the GCNNF.

EXPERIMENTAL SECTION

Fabrication of GCNNF. An amount of 1 g of melamine was dissolved in 20 mL of ethanol to make a saturated solution. Then 60 mL of 0.2 M HNO_3 was added to the above solution, and after stirring for 10 mins it was washed with ethanol and dried at 60 °C for 12 h. A white color powder was obtained which was annealed at 450 °C for 2 h in the CVD furnace in an alumina tube at a ramp rate of 10 °C min^{-1}. The bulk was prepared by polymerization of melamine at high temperature. In short, 1 g of melamine was taken in an alumina crucible and heated at 550 °C for 2 h with a ramp rate of 3 °C min^{-1}. The obtained yellow products were bulk g-C_3N_4 (GCN).

Samples were characterized by scanning electron microscopy (SEM, Hitachi S-4800), X-ray diffraction (XRD Philips X'Pert Pro MPD), X-ray photoelectron spectra (XPS, Thermo Scientific, Escalab 250Xi), Fourier transform infrared (FTIR) spectroscopy (EXCALIBUR FTS3100), UV absorption spectroscopy (Hitachi FL-4500 spectro-

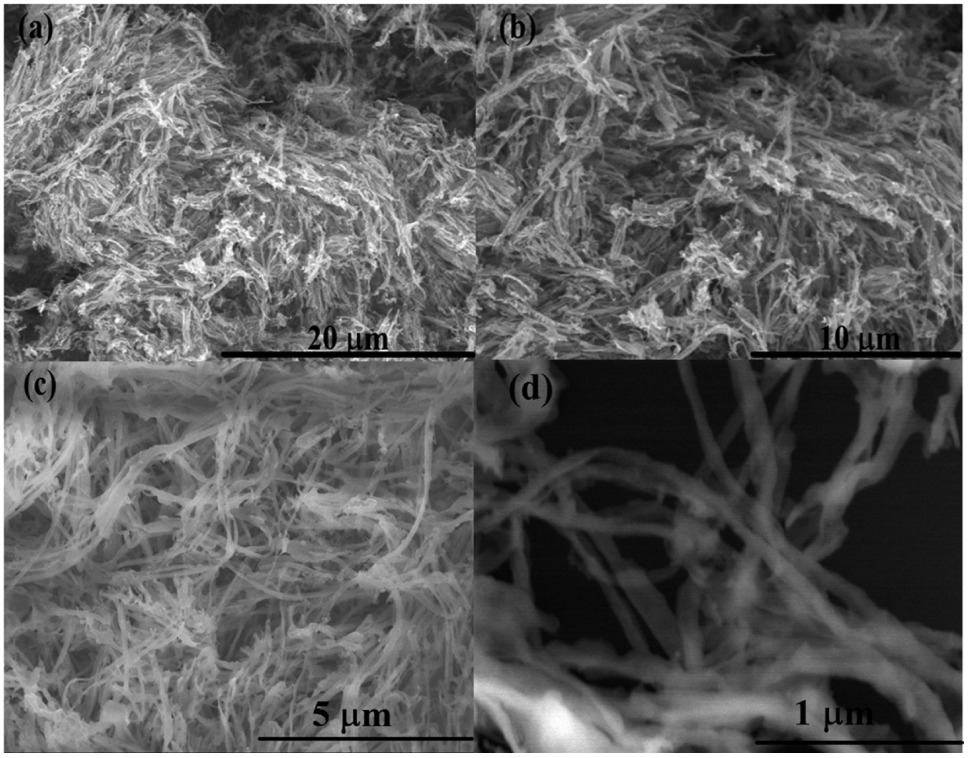

Figure 1. (a,b) Low-magnification SEM images of GCNNF and (c,d) high-magnification SEM images of GCNNF.

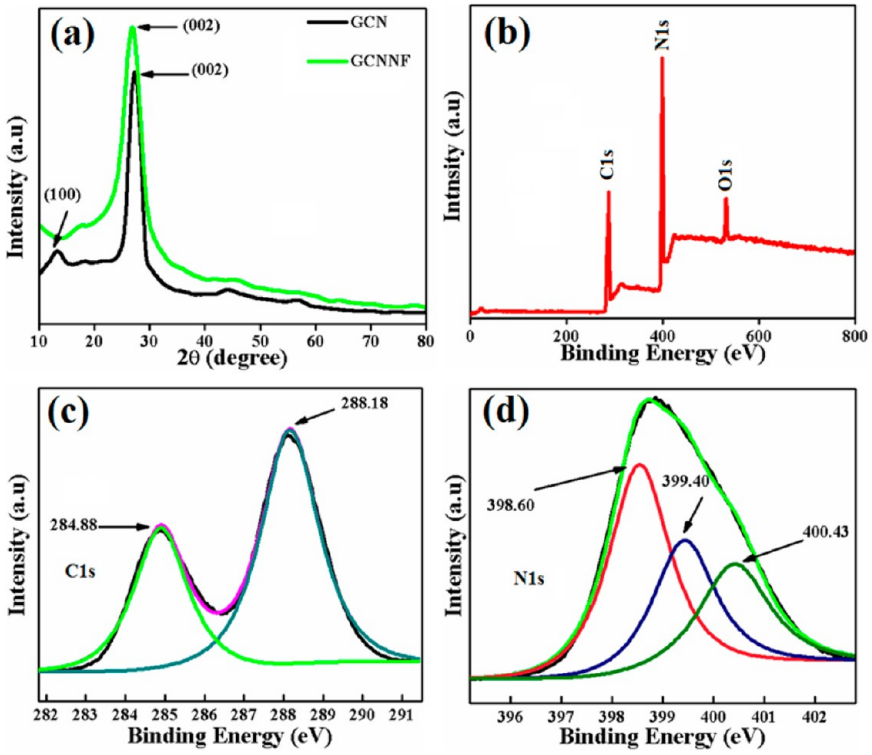

Figure 2. (a) XRD patterns of GCNNF and GCN. (b) XPS survey spectrum of GCNNF. (c) High-resolution C 1s of GCNNF. (d) High-resolution N 1s of GCNNF.

fluorometer), and photoluminescence (PL) absorption spectroscopy (Hitachi U-4100 spectrofluorometer).

Preparation of Electrodes. The GCNNF 85%, activated carbon 10%, and polytetrafluoroethylene (PTFE) 5% were mixed with ethanol, then pasted on nickel foam (5 cm × 1 cm) and dried at 60 °C for 12 h. Ag/AgCl (saturated KCl solution) electrode and platinum wires were used as the counter and reference electrodes, respectively. The electrochemical behavior of the working electrode was analyzed in 0.1 M Na_2SO_4 electrolytes in a three-electrode cell.

Photocatalytic Test. The photocatalytic activities of GCN and GCNNF were evaluated by the degradation of RhB under visible light. A 500 W Xenon lamp was used as a visible light source. To study the

dx.doi.org/10.1021/am405076b | ACS Appl. Mater. Interfaces 2014, 6, 1258−1265

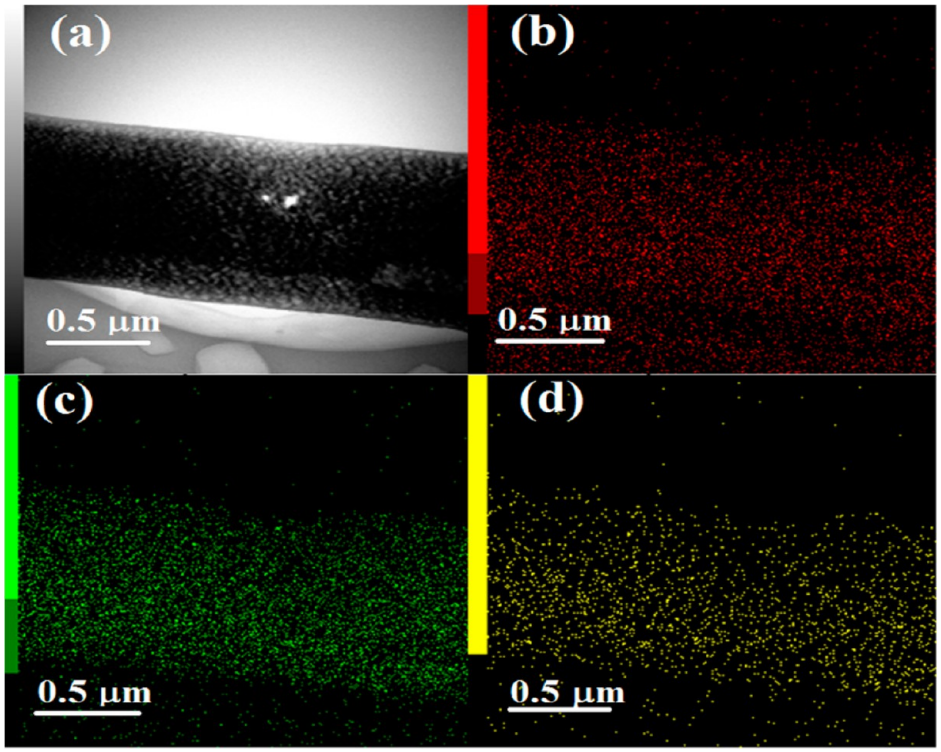

Figure 3. (a) Elemental mapping of GCNNF, (b) carbon, (c) nitrogen, and (d) oxygen.

concentration of RhB in solution, an UV−vis−NIR (Hitachi U-4100) spectrophotometer was used. For photocatalytic tests, 0.40 L of 0.01 M RhB was taken in a glass beaker, and 0.1 g of samples was dissolved in this solution. Prior to irradiation, the solution was magnetically stirred in the dark for 50 mins to obtain the saturated absorption of RhB onto the catalysts, and then this solution was brought into visible light. At irradiation time intervals of every 15 mins, the suspensions were collected and then centrifuged to remove the photocatalyst particles. The initial concentration (C_0) was the maximum absorption peak of the RhB at 554 nm. For stability measurement the same material was evolved from the solution, and the above-mentioned steps were repeated for second and third time.

RESULTS AND DISCUSSION

Characterization of the GCNNF. The synthesis reaction of the GCNNF is described in Scheme 1, which clearly depicts that reaction is a combination of poly addition and poly condensation. In the first step, nitric acid activates the melamine to form the heptazine or cyamelurine through the elimination of ammonia. Furthermore, the condensation of these units develops a polymeric network to produce GCNNF at higher temperature. Here, the basic units are strongly bonded with each other through the covalent bonds that solve the major hurdle of melamine used to produce carbon nitride as melamine is prone to sublimation at comparatively higher temperature. Here nitric acid activates the melamine to form a bigger unit of heptazine, which further polymerizes to form melon and melon sheets in the presence of polar solvents which tend to make the fibrous structure with unique properties. These sheets are held together through the hydrogen bonding or weak van der Waals attractions.

A scanning electron microscope (SEM) is used to investigate the textural structure and morphology of GCNNF as shown in Figure 1. Figure 1(a,b) shows the typical SEM images of the sample at low magnification. From these SEM images it is clear that GCNNF grew in fibrous morphology having very dense and uniform structure with an average diameter of 100 nm and 20 μm in length. To further confirm the fibrous morphology of as-synthesized GCNNF, high-magnification SEM studies were carried out. It is obvious from Figure 1(c,d) that the entire sample consists of uniform and distinctive nanofibers with a smooth surface.

X-ray diffraction (XRD) was conducted to identify phase and structural characterizations of GCN and GCNNF as shown in Figure 2(a). There are two distinct diffraction peaks for GCN at 13.1° and 27.3°. The low-angle reflection peak at 13.1° was identified as (100) corresponding to d = 0.676 nm resulting from the trigonal nitrogen linkage of tri-*s*-triazine units. A strong peak at 27.3° corresponds to d = 0.326 nm due to long-range interplanar stacking of aromatic systems recognized as (002). These two XRD peaks are in good agreement with reported GCN.[4,6] There is only one peak for GCNNF at 27.3° that corresponds to a distance d = 0.326 nm due to long-range interplanar stacking of aromatic systems recognized as the (002).[4,6,18]

To investigate the chemical compositions and the nature of chemical bonding of constituent elements on the surface of prepared GCNNF, X-ray photoelectron spectroscopy (XPS) was conducted as shown in Figure 2(b−d). The existence of core levels of carbon and nitrogen confirms high purity of product as shown in Figure 2(b). A small amount of oxygen is also identified during the XPS studies which might be due to surface adsorption of oxygen. The GCNNF has a C/N ratio of 0.82, higher than the stoichiometry of the theoretical material (C/N = 0.75). Figure 2(c) represents the high-resolution C 1s XPS spectrum of GCNNF. The C 1s peak of GCNNF can be deconvoluted into two peaks at 284.88 and 288.18 eV, which specify that two different chemical states of carbon exist in GCNNF. The peak at 284.88 eV is due to sp^2 hybridization of C bonded to N in an aromatic ring, whereas the second peak at 288.18 eV corresponds to C−N bonding in GCNNF.[7−10]

dx.doi.org/10.1021/am405076b | ACS Appl. Mater. Interfaces 2014, 6, 1258−1265

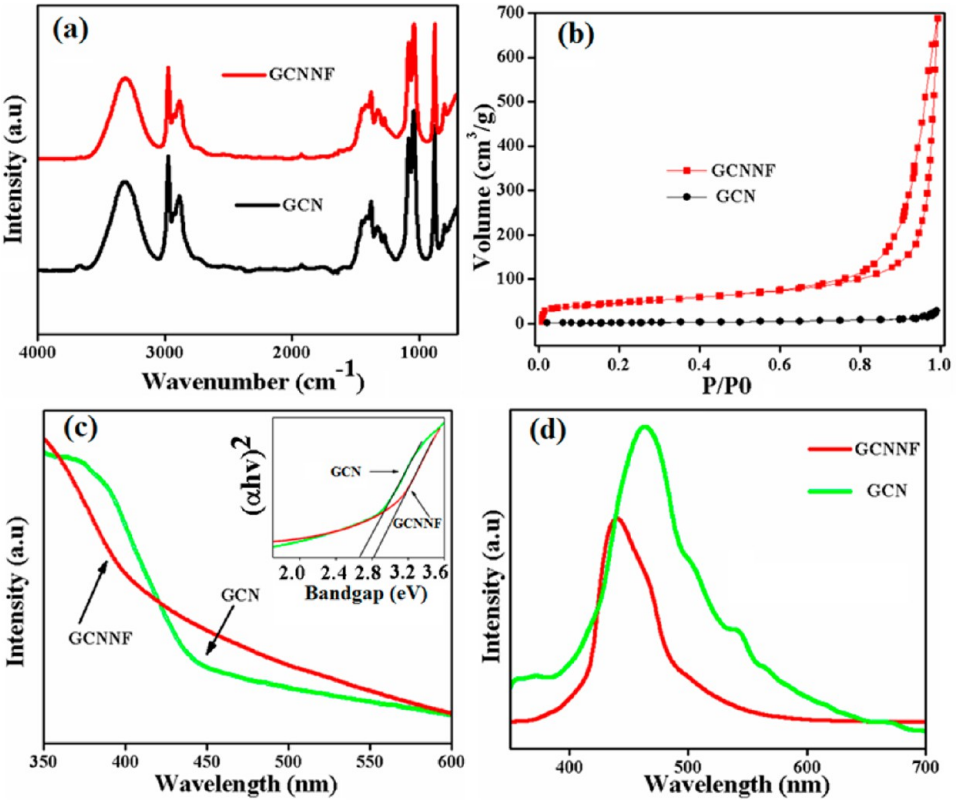

Figure 4. (a) FTIR spectra, (b) N_2 adsorption−desorption isothermal curves, (c) UV spectra and bandgap, and (d) PL spectrum of GCNNF and GCN.

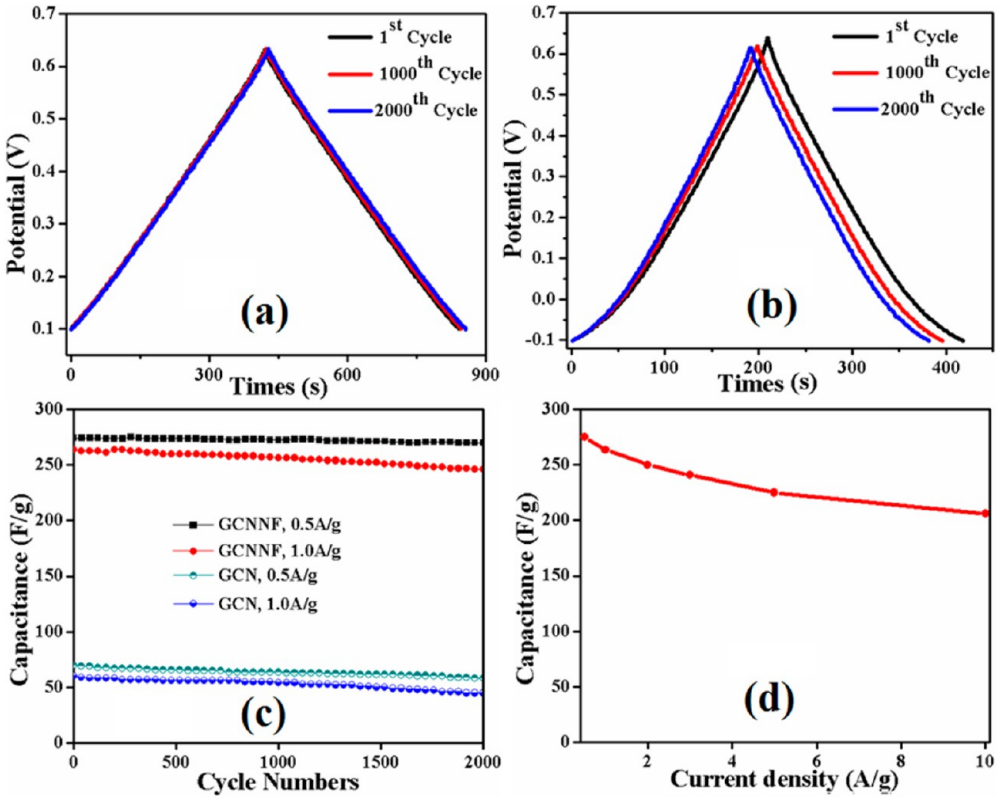

Figure 5. (a) 1st, 1000th, and 2000th charging−discharging curves within a potential window of −0.1 to 0.7 V for current density 0.5 A g^{-1} of GCNNF. (b) 1st, 1000th, and 2000th charging−discharging curves within a potential window of −0.1 to 0.7 V for current density 1.0 A g^{-1} of GCNNF. (c) Cyclic performance of GCNNF and GCN at 0.5 and 1 A g^{-1}. (d) Capacitance of GCNNF as a function of current density.

dx.doi.org/10.1021/am405076b | ACS Appl. Mater. Interfaces 2014, 6, 1258−1265

Similarly, N 1s has been resolved to three peaks at 398.60, 399.4, and 400.43 eV which correspond to three different types of nitrogen states as presented in Figure 2(d). The peaks at 398.60, 399.4, and 400.43 eV confirm the existence of pyridinic, pyrrolic, and graphitic nitrogen, respectively, in the product.[17,22]

The elemental mapping analysis (Figure 3) of GCNNF clearly shows the spatial distribution of carbon and nitrogen, and a small amount of oxygen is also present in GCNNF that is consistent with XPS results.

Fourier transform infrared spectroscopy (FTIR) was utilized to characterize the chemical bonds present in GCN and GCNNF. Figure 4(a) shows the FTIR spectra of GCN and GCNNF which confirm the presence of two main bands in the products. The absorption peaks which range from 800 to 1600 cm^{-1} are a strong indication of the heterocycles present in GCN, and these peaks are due to the breathing mode of *s*-triazine, sp^3 C−N bonds, and sp^2 C═N. Furthermore, these results are consistent with XRD and XPS results of GCNNF.[7−10] The peaks because of the stretching vibration modes of NH and NH_2 groups are observed in the range of 3300−3500 cm^{-1} in both samples.[7,9,22]

The surface areas of GCNNF and GCN were determined through the Brunauer−Emmett−Teller (BET) equation in the relative pressure range (P/P_0) of 0−1. The surface area of GCNNF is found to be much higher (∼165 m^2 g^{-1}) as compared to that of GCN (∼4 m^2 g^{-1}). The BET adsorption curves as a function of P/P_0 for GCNNF and GCN are presented in Figure 4(b).

The optical properties of GCN and GCNNF were studied using UV spectrophotometer and photoluminescence (PL) measurements at room temperature as a function of wavelength. The optical characteristics like absorption coefficient and bandgap are important parameters for photocatalysts. So, we measured the optical bandgap and absorption coefficient using the absorbance data. The UV−vis diffuse reflectance spectrum of GCN and GCNNF features typical semiconductor-like absorption which can be seen in Figure 4(c). GCN has a band edge at 465 nm corresponding to 2.67 eV, while GCNNF has a band edge at 443 nm corresponding to a bandgap at 2.80 eV that indicates a slight blue shift by 0.13 eV compared to GCN. This is due to a more perfect packing, electronic coupling, and quantum confinement effect that shifts conduction and valence band edges. The PL emission peak for GCN shows a strong peak at 464 nm, whereas for GCNNF an emission peak is observed at 445 nm as shown in Figure 4(d). Both peaks are coherent with their bandgap measurements of the respective products. It belongs to a blue-violet light band that indicates the existence of the π state in GCNNF.[7−10] The larger bandgap by 0.13 eV of the GCNNF is also confirmed by PL. From Figure 5(d) it is also proved that PL intensity of GCN is high in comparison to that of GCNNF which indicates the slow recombination rate of photogenerated electrons and holes. The decrease of PL intensity is because of the defects in crystal structure that reduce the strength of fluorescence peaks. These defects are the recombination centers for electrons and holes generated during photocatalysis. Therefore, a decrease in the number of defects in GCNNF ultimately increases its photocatalytic performance.[23] It is assumed that the high energy level bandgap would obtain the thermodynamically enhanced reduction and oxidation power in photodegradation of the dye. The charge-transfer rate between GCNNF and redox species in solution also depends on such an energy level relationship.[24]

Electrochemical Performance. Figure 5(a) shows the 1st, 1000th, and 2000th charge−discharge curves of GCNNF in 0.1 M aqueous solution of Na_2SO_4 at a current density of 0.5 A g^{-1}. The time duration difference among the charge−discharge of the 1st and 2000th cycle is very small which indicates extraordinary stability of the GCNNF electrode. Similarly, the time difference of the 1st, 1000th, and 2000th charge−discharge curves of GCNNF tested at a current density of 1 A g^{-1} is also small which further confirms the high stability of the GCNNF electrode as shown in Figure 5(b). Furthermore, it is observed that the discharging time of GCNNF is large at lower current density (0.5 A g^{-1}) as compared to higher current density (1 A g^{-1}).

The cyclic performance of GCNNF and GCN is delineated in Figure 5(c). The electrode composed of GCNNF shows a specific capacitance of 275 F g^{-1} at a current density of 0.5 A g^{-1} for the 1st cycle and 270 F g^{-1} for the 2000th cycle that possess its remarkable long-term cycling stability. On the other hand, in comparison to GCNNF, GCN exhibits very low specific capacitance of 71 F g^{-1} at the current density of 0.5 A g^{-1} for its first cycle which is 3.87 times lower than that of GCNNF. The cycling performance is an important factor to determine the practical applications of an electrode material in real supercapacitors. The specific capacitance of GCNNF is 263.75 F g^{-1} at the current density of 1 A g^{-1} for the first cycle, and it keeps its capacitance of 246 F g^{-1} even after 2000 cycles. Furthermore, it proves its excellent retention capability of 98.18% at 0.5 A g^{-1} and 93.2% at 1 A g^{-1} of the GCNNF electrode. Such a high retention capability shows the structural stability of the GCNNF during the electrochemical process. The specific capacitance of GCNNF is much better than several reported carbon-based materials like nitrogen-enriched nanocarbons, nitrogen-enriched carbon, MWCNTs, CNTs, oxygen-rich carbon, CNTs/N-carbon, nitrogen-doped carbon nanocage, nitrogen-doped graphene, nitrogen-doped carbon, porous 3D graphene, and g-C_3N_4 hybridized α-Fe_2O_3 hollow microspheres.[25−34]

Figure 5(d) shows specific capacitance of the GCNNF electrode as a function of current density. From Figure 4(d) it is obvious that the GCNNF retains a high capacitance of 206 F g^{-1} at a current density of 10 A g^{-1} with the excellent capacitance retention of 89.5%, which confirms that the GCNNF has a good rate capability. At low current density (0.5 A g^{-1}), the electrolyte ion can access the maximum surface of the GCNNF, hence a higher specific capacitance has been achieved. When the current density increases (10 A g^{-1}), the effective interaction between the electrode and ions is reduced; therefore, specific capacitance is also reduced.

On the basis of exceeding discussion, it can be concluded that GCNNFs are suitable and promising supercapacitor electrode materials. The good specific capacitance of GCNNF electrodes could be attributed to the existence of nitrogen. The presence of nitrogen in GCNNF is helpful to enhance the capacitance in different ways: (1) it provides various active reaction sites, (2) improves the surface wettability of GCNNF which is useful for the electrolyte into the inner layer of the carbons, (3) increases the electron donor/acceptor characteristics, (4) improves the wettability with the electrolytes and consequently enhances the mass transfer efficiency, and (5) provides a large additional pseudo-capacitance. Secondly, high capacitance is based on large surface areas of GCNNF that

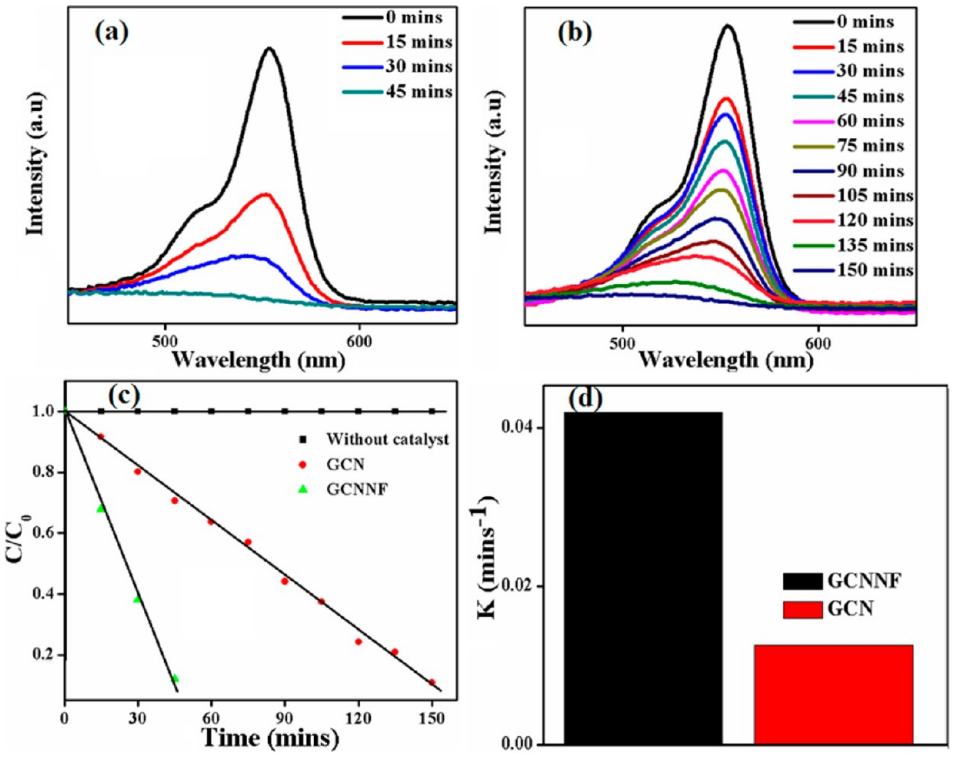

Figure 6. (a) Photodegradation of RhB by using GCNNF. (b) Photodegradation of RhB by using GCN. (c) C/C_0 of GCN, GCNNF, and without catalyst. (d) First-order rate constant k (min^{-1}) of GCN and GCNNF.

provide the advantage of large electrode−electrolyte contact and improved electrolyte ion transport. Lastly, the high capacitance of GCNNF is because of the easily tailorable structure of GCNNF.[17,25,34]

Photocatalytic Performance. Figure 6 shows the photocatalytic activity of GCNNF and GCN. Figure 6(a,b) shows the decrease in the concentration of RhB as a function of irradiation time. GCNNF was able to completely degrade RhB in an irradiation time of 45 mins, with 60% of the RhB being degraded in the initial 15 mins, although GCN required 150 min for the complete degradation of the same concentration of RhB. In Figure 6(c), the relationship between C/C_0 and time of GCN, GCNNF, and sample without any catalyst are shown. The sample without catalyst shows almost no change with time under visible light. Thus, it is obvious that RhB is stable under visible light if there is no photocatalyst involved. The graph showed that C/C_0 decreased linearly with the course of time. Figure 6(d) shows the first-order rate constant k ($mins^{-1}$) measurements of GCNNF and GCN for RhB. The measured k value of GCNNF is 0.0412 min^{-1} as compared to GCN (0.0114 min^{-1}). However, the k value of GCNNF is almost 4 times higher than that of GCN. The higher photocatalytic activity of GCNNF corresponds to its large surface area and fewer textural structure defects.

It is significant to point out that the stability of a photocatalyst during photocatalytic reaction is an essential factor for its practical application. Thus, to observe the stability of GCNNF, a recycling reaction was carried out as shown in Figure 7. Similarly, a second cycle test was performed by using the same sample, while RhB concentration was kept the same as used in a previous test. Thus, the solution was again kept in the dark for 50 min to reach its saturated point and then exposed to visible light. It took the same time without any significant loss of efficiency; the third cyclic efficiency was also

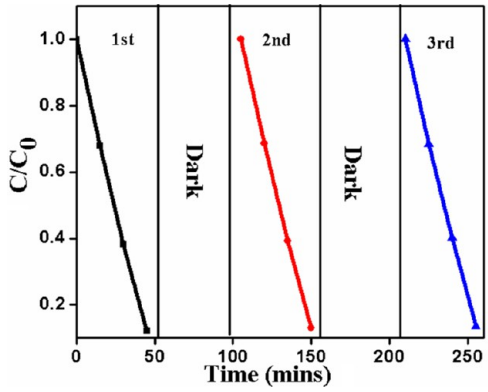

Figure 7. Stability test of GCNNF for three consecutive cycles.

similar. The degradation efficiency of GCNNF has decreased only 2% after three successive cycles which indicates good stability and reusability of GCNNF.

The bandgap of the GCNNF reveals that the reactive oxidative nature of photocatalytic reaction is because of the superoxide radicals, produced by photogenerated electrons of GCNNF. The hydroxyl radicals are produced by the photogenerated electron induced in different steps of the reduction of oxygen.[24] Therefore, the addition of 1 mL of H_2O_2 into the GCNNF and RhB solution increases its k value. Furthermore, the excellent photodegradation capability of GCNNF is also based on its large surface area and higher aspect ratio which provide more reactive sites for reaction. It reduces the recombination probability of photoexcited charge carriers and increases the transport of charges.

dx.doi.org/10.1021/am405076b | ACS Appl. Mater. Interfaces 2014, 6, 1258−1265

CONCLUSIONS

In summary, we have successfully prepared GCNNF without any hard or soft template by a green and facile method. The as-prepared high surface area graphitic carbon nitride nanofibers have a great influence on improving optical, electrochemical, and photocatalytic properties of the bulk-GCN. It was found that GCNNF exhibits good electrochemical performance as electrodes for supercapacitors and excellent photocatalytic activity toward photodegradation of RhB. The extraordinary specific capacitance for a carbon material (excellent capacity retention of 89.5% for 2000 cycles at high charge/discharge rates) and excellent photocatalytic activity are mainly because of the existence of nitrogen, higher surface area, suitable bandgap, fewer textural structure defects, and easily tailorable structure of GCNNF. The above-mentioned unique properties induce that GCNNF is also a promising candidate for hydrogen production and oxygen reduction reaction for fuel cells that are under progress in our laboratories.

AUTHOR INFORMATION

Corresponding Author

*E-mail: cbcao@bit.edu.cn. Tel.: +86 10 6891 3792. Fax: +86 10 6891 2001.

Notes

The authors declare no competing financial interest.

ACKNOWLEDGMENTS

This work was supported by National Natural Science Foundation of China (21371023, 50972017), the Research Fund for the Doctoral Program of Higher Education of China (20101101110026), and 21371023 to NFSC funding.

REFERENCES

(1) Lijima, S. *Nature* **1991**, *354*, 56−58.
(2) Younan, X.; Peidong, Y.; Yogang, S.; Yiying, W.; Brian, M.; Byron, G.; Yadong, Y.; Franklin, K.; Haoquan, Y. *Adv. Mater.* **2003**, *15*, 353−389.
(3) Butt, F. K.; Cao, C. B.; Waheed, S. K.; Safdar, M.; Fu, X.; Tahir, M.; Idrees, F.; Ali, Z.; Nabi, G.; Yu, D. *CrystEngComm* **2013**, *15*, 2106−2112.
(4) Jun, G.; Yong, Z.; Zhaosheng, L.; Shicheng, Y.; Nanyan, W.; Zhigang, Zou. *Nanoscale* **2012**, *4*, 3687−3692.
(5) Tahir, M.; Cao, C. B.; Butt, F. K.; Idrees, F.; Mahmood, N.; Ali, Z.; Aslam, I.; Tanveer, M .; Rizwan, M.; Mahmood, T. *J. Mater. Chem. A* **2013**, *1*, 13949−13955.
(6) Tahir, M.; Cao, C. B.; Butt, F. K.; Butt, S.; Idrees, F.; Ali, Z.; Aslam, I.; Tanveer, M.; Mahmood, A.; Mahmood, N. *CrystEngComm* **2013**, DOI: 10.1039/C3CE42135J.
(7) Wang, X. C.; Maeda, K.; Thomas, A.; Takanabe, K.; Xin, G.; Carlsson, J. M.; Domen, K.; Antonietti, M. *Nat. Mater.* **2009**, *8*, 76−80.
(8) Yin, L. W.; Bando, Y.; Li, M. S.; Liu, Y. X.; Qi, Y. X. *Adv. Mater.* **2003**, *15*, 1840−1844.
(9) Jun, G.; Yong, Z.; Zhao, S. L.; Shicheng, Y.; Nanyan, W.; Zhigang, Z. *Nanoscale* **2012**, *4*, 3687−3692.
(10) Ping, N.; Gang, L.; Hui, M. C. *J. Phys. Chem. C* **2012**, *116*, 11013−11018.
(11) Bin, X.; Hui, D.; Mo, C .; Gaoping, C.; Yusheng, Y. *J. Mater. Chem. A* **2013**, *1*, 4565−4570.
(12) Zhang, L. L.; Zhou, R.; Zhao, X. S. *J. Mater. Chem.* **2010**, *20*, 5983−5992.
(13) Zhang, L. L.; Zhao, X.S. *Soc. Rev.* **2009**, *38*, 2520−2531.
(14) Long, H.; Xianglong, L.; Linjie, Z. *Adv. Mater.* **2013**, *25*, 3899−3904.
(15) Tingting, L.; Guangwen, Y.; Jing, W.; Yuanyuan, Z.; Heyou, H. *J. Solid State Electrochem.* **2013**, *17*, 2651.
(16) Yu, D. S.; Xue, Y. H.; Dai, L. M. *J. Phys. Chem. Lett.* **2012**, *3*, 2863−2870.
(17) Xu, L.; Xia, J.; Xu, H.; Yin, S.; Wang, K.; Huang, L.; Wang, L.; Li, H. *J. Power Sources* **2013**, *245*, 866−874.
(18) Jinshui, Z.; Fangsong, G.; Xinchen, W. *Adv. Funct. Mater.* **2013**, *23*, 3008−3014.
(19) Yan, S. C.; Lv, S. B.; Li, Z. S.; Zou, Z. G. *Dalton Trans.* **2010**, *39*, 1488−1491.
(20) Zhou, X. S.; Peng, F.; Wang, H. J.; Yu, H.; Fang, Y. P. *Chem. Commun.* **2011**, *47*, 10323−10325.
(21) Siyuan, Y.; Wuyi, Z.; Chunyu, G.; Xiaotang, L.; Yueping, F.; Zesheng, L. *RSC Adv.* **2013**, *3*, 5631−5638.
(22) Xinjiao, B.; Jie, L.; Cao, C.B. *Appl. Surf. Sci.* **2010**, *256*, 2327−2331.
(23) Yipeng, Z.; Liping, L.; Ying, Z.; Haifeng, L.; Guangshe, L.; Xiangfeng, G. *RSC Adv.* **2013**, *3*, 13646−13650.
(24) Young, S. J.; Eun, Z. L.; Xinchen, W.; Won, H. H.; Galen, D. S.; Arne, T. *Adv. Funct. Mater.* **2013**, *23*, 3661−3667.
(25) Xiaoqing, Y.; Dingcai, W.; Xiaomei, C.; Ruowen, F. *J. Phys. Chem.C* **2010**, *114*, 8581−8586.
(26) Lota, G.; Lota, K.; Frackowiak, E. *Electrochem. Commun.* **2007**, *9*, 1828−1832.
(27) Jurewicz, K.; Babel, K.; Pietrzak, R.; Dupleux, S.; Wachowska, H. *Carbon* **2006**, *44*, 2368−2375.
(28) Jurcakova, D. H.; Masaya, K.; Soshi, S.; Hiroaki, H.; Zong, H. Z.; Gao, Q. L. *Adv. Funct. Mater.* **2009**, *19*, 1800−1809.
(29) Frackowiak, E.; Lota, G.; Machnikowski, J.; VixGuterl, C.; Beguin, F. *Electrochim. Acta* **2006**, *51*, 2209−2214.
(30) Pinero, E. R.; Leroux, F.; Beguin, F. *Adv. Mater.* **2006**, *18*, 1877−1882.
(31) Li, W.; Chen, D.; Li, Z.; Shi, Y.; Wan, Y.; Huang, J.; Yang, J.; Zhao, D.; Jiang, Z. *Electrochem. Commun.* **2007**, *9*, 569−573.
(32) Beguin, F. S.; Lota, K.; Frackowiak, G. *Adv. Mater.* **2005**, *17*, 2380−2384.
(33) Chen, L. F.; Zhang, X. D.; Liang, H. W.; Kong, M.; Guan, Q. F.; Chen, P.; Wu, Z. Y.; Yu, S. H. *ACS Nano* **2012**, *6*, 7092−7102.
(34) Long, Z.; Fan, Z.; Xi, Y.; Guankui, L.; Yingpeng, W.; Tengfei, Z.; Kai, L.; Yi, H.; Yanfeng, M.; Ao, Y.; Yongsheng, C. *Sci. Rep.* **2013**, *3*, 1408, 1−9.